DOE/ET-53088-638 IFSR #638

Constructing Symplectic Maps for Application to Magnetostatics and Hamiltonian Mechanics

PETER M. ABBAMONTE
Department of Physics
The University of Texas at Austin
Austin, Texas 78712
and
P.J. MORRISON
Department of Physics and Institute for Fusion Studies
The University of Texas at Austin
Austin, Texas 78712

June 1994

Constructing Symplectic Maps for Application to Magnetostatics and Hamiltonian Mechanics

Peter M. Abbamonte
Department of Physics
The University of Texas at Austin
Austin, TX 78712
and
P. J. Morrison
Department of Physics and Institute for Fusion Studies
The University of Texas at Austin
Austin, Texas 78712

Abstract

Various methods of constructing two-dimensional, area-preserving maps of general Hamiltonian systems are explored. Emphasis is on constructing maps with a given set of fixed points, a given invariant curve, or a given topology, and also on guaranteeing integrability. One method is used to find an integrable Poincáre map for the field lines in a tokamak with a single null-divertor where the q-profiles can be arbitrarily chosen.

I. Introduction: Hamiltonian Systems and Symplectic Maps

A. Hamiltonian surfaces of section

The most informative way to observe the time evolution of a Hamiltonian system is to view its trajectory in phase space. However, since the phase space for a Hamiltonian with N degrees of freedom is $2N$ dimensional, for any system with multiple degrees of freedom, the trajectories are impossible to depict. Even surfaces of constant energy in a two degree-of-freedom system (which are three-dimensional) require awkward, perspective drawings for viewing.

To deal with this, the "surface of section" (also called the "Poincáre section") was proposed by Poincáre (1892) as a method for viewing two-dimensional cross-sections of general phase space trajectories. Use of this method goes as follows: A single coordinate x^i is chosen from the collection of coordinates, and a separate two-dimensional plot is prepared with this coordinate on one axis and its conjugate momentum p_i on the other. Each of the remaining coordinates and momenta is assigned a constant value, thereby specifying a $2N-2$ dimensional surface in the $2N$ dimensional space. Hamilton's equations are then integrated forward in time, and every time the trajectory pierces this $2N-2$ surface (if does at all), the values of x^i and p_i are plotted (Fig. 1). The result is a collection of points in the plane that can reveal important topological features of the trajectory and of the energy surfaces.

B. Expressing surfaces of section as maps

Under the fortuitous circumstances that the trajectory of a Hamiltonian can be solved and expressed explicitly, the surfaces of section can be expressed by a discrete pair of equations,

simply called a "map," of the form

$$\begin{aligned} y_{n+1} &= f(x_n, y_n) \\ x_{n+1} &= g(x_n, y_n) \ . \end{aligned} \tag{1}$$

Here, initial conditions are chosen from the points available on the specified surface of section, the equations are iterated, and points are plotted to produce a collection of points like that shown in Fig. 1. Maps are more efficient for viewing phase space topology (especially when looking at many different trajectories) than finding the surface of section by numerically integrating the trajectory.

Since Hamilton's equations exhibit phase space volume preservation (Liouville's theorem), a map of this form will always be area preserving (i.e. will have a unitary Jacobian determinant). A two-dimensional map that is area preserving is said to be "symplectic."

If one wishes to study a system that is known to be Hamiltonian, but an explicit Hamiltonian for it is not known, a map can sometimes be a good starting point. If the qualitative behavior of the system is known, often the topology of the phase space, and consequently its surfaces of section, can be approximately guessed (i.e. "it should have a closed region over here, with a fixed point here, and such and such an amount of stochasticity etc."). Since the surface of section is directly related to the Hamiltonian, if a surface of section map can be found that has the desired topology, a Hamiltonian can sometimes be guessed. Once the Hamiltonian is found, the system is open for study using all the tools of Hamiltonian mechanics. For example, one can perturb the Hamiltonian, propagate the perturbation back into the map and see how this affects the surfaces of section.

The ensuing discussion centers around methods for finding symplectic maps with desired qualitative features (i.e. desired fixed points, invariant curves, topology etc.) so that such methods can be used.

II. Constructing Maps

A. Simple maps with specified stationary points

Given a pair of transformation equations of the form given in Eq. (1), a *fixed point* of period N is defined to be a point that satisfies the condition

$$\begin{aligned} x_n &= x_{n+N}(x_n, y_n) \\ y_n &= y_{n+N}(x_n, y_n) \end{aligned} \tag{2}$$

where (x_{n+N}, y_{n+N}) is the point obtained after applying N successive iterations of the transformation equations on the point (x_n, y_n). There could be many points that satisfy this condition, so call them (x_i^*, y_i^*).

Fixed points come in two types, o-points or "stable" fixed points and x-points or "unstable" fixed points. Stable and unstable refer to the behavior of initial conditions in the vicinity of a fixed point during successive applications of the iteration. Points that stay in the vicinity are stable and those that diverge exponentially are unstable. A point can be identified as one or the other using the following procedure: Write the transformation from (x_n, y_n) to (x_{n+N}, y_{n+N}) in the form of column vectors

$$\begin{pmatrix} x_{n+N} \\ y_{n+N} \end{pmatrix} = \begin{pmatrix} x_{n+N}(x_n, y_n) \\ y_{n+N}(x_n, y_n) \end{pmatrix} . \tag{3}$$

Expand this expression around the fixed point (x_i^*, y_i^*) to get the series

$$\begin{pmatrix} x_{n+N} \\ y_{n+N} \end{pmatrix} = \begin{pmatrix} x_{n+N}(x_i^*, y_i^*) \\ y_{n+N}(x_i^*, y_i^*) \end{pmatrix} + \begin{pmatrix} \frac{\partial x_{n+N}}{\partial x_i^*} & \frac{\partial x_{n+N}}{\partial y_i^*} \\ \frac{\partial y_{n+N}}{\partial y_i^*} & \frac{\partial y_{n+N}}{\partial y_i^*} \end{pmatrix} \begin{pmatrix} dx \\ dy \end{pmatrix} + \cdots . \tag{4}$$

Here, $x_{n+N} = x_i^* + dx$ and $y_{n+N} = y_i^* + dy$. Finally, insert the same fixed point (x_i^*, y_i^*) into (4) and discard higher order terms to get the matrix equation

$$\begin{pmatrix} \frac{\partial x_{n+N}}{\partial x_i^*} & \frac{\partial x_{n+N}}{\partial y_i^*} \\ \frac{\partial y_{n+N}^*}{\partial x_i^*} & \frac{\partial y_{n+N}^*}{\partial y_i^*} \end{pmatrix} \begin{pmatrix} dx \\ dy \end{pmatrix} = T^N \begin{pmatrix} dx \\ dy \end{pmatrix} = 0 . \tag{5}$$

Since the matrix T^N is a 2×2, it has two eigenvalues λ_1 and λ_2, and these contain information about the stability of (x_i^*, y_i^*). Because of the area preservation condition $\lambda_1 = 1/\lambda_2$. If λ_1 and λ_2 are real and distinct, the fixed point is unstable (i.e. an x-point), and if they are complex and distinct, the point is stable (i.e. an o-point). If both eigenvalues are equal to 1 (which incidentally is generally not the case for low-order fixed points), the point is said to be "parabolic" and is probably a point on a closed, integrable invariant curve.

Now if one wishes to describe a physical system (with an unknown Hamiltonian) of which the most important feature is the existence of a number of fixed points. It would be desirable to construct a map with such fixed points to represent the surfaces of section (so that a Hamiltonian might be found). What follows are a few simple methods for doing this.

1 Direct method

Suppose the desired surface of section has fixed points (x_i^*, y_i^*), each of which is specified in advance to be either stable or unstable. Let the stability of the i^{th} fixed point be represented by the eigenvalues λ_i^1 and λ_i^2, which are chosen in advance arbitrarily to set the desired stability.

One seeks a pair of transformation equations of the form

$$\begin{aligned} x_{n+N} &= x_{n+N}(x_n, y_n) \\ y_{n+N} &= y_{n+N}(x_n, y_n) \end{aligned} \tag{6}$$

that are consistent with the desired fixed points and their stability. The stationarity condition is

$$\begin{aligned} x_i^* &= x_{i+N}(x_i^*, y_i^*) \\ y_i^* &= y_{i+N}(x_i^*, y_i^*) \ , \end{aligned} \tag{7}$$

and the stability condition (using area preservation) is

$$(\lambda_i^1)^2 - \lambda_i^1 \left(\frac{\partial y_{i+N}}{\partial y_i} + \frac{\partial x_{i+N}}{\partial x_i} \right) + 1 = 0 \ , \qquad \lambda_i^2 = 1/\lambda_i^1 \ . \tag{8}$$

If k is the number of desired fixed points, equations (7) and (8) constitute $4k$ coupled, algebraic equations that put constraints on Eqs. (6) that can be solved simultaneously to achieve the desired fixed points. Aside from $4k$ constraints, Eqs. (6) can be chosen to have any form that is convenient and the stability of the points (x_i^*, y_i^*) is still guaranteed.

2 Simplification through constraint of form

Equations (7) and (8) do not uniquely identify a pair of mapping equations. These are only $4k$ constraints (which implicitly include area preservation) on a pair of functions that are otherwise completely general. Therefore, given a set of desired fixed points (x_i^*, y_i^*), there is an unaccountably infinite number of maps that can provide these fixed points with their specified stability. Therefore, in practical terms it is usually necessary to pick a form for the transformation (6) before proceeding to solve (7) and (8).

For example, if the transformation is chosen to have the linear form

$$\begin{aligned} x_{n+N} &= ax_n + by_n \\ y_{n+N} &= cx_n + dy_n \end{aligned} \tag{9}$$

then the constraint equations come out to be

$$\begin{aligned} x_n &= ax_n + by_n \\ y_n &= cx_n + dy_n \end{aligned} \tag{10a}$$

and

$$(\lambda_i^1)^2 - \lambda_i^1(a+d) + 1 = 0\ , \qquad \lambda_i^2 = 1/\lambda_i^1\ . \tag{10b}$$

These constitute $4k$ equations to solve for the coefficients a, b, c and d. Effectively, (9) reduces the number of available degrees of freedom from infinity to 4. Consequently, this map can accommodate only one fixed point (in addition to the origin) so $k = 1$. This means that the choice of (9) as a constraint was a pretty strong one (perhaps too strong for any practical use) but it illustrates the simplicity and efficacy of the method.

3 Classical potential method: kicking

Suppose one is given a simple one-dimensional Hamiltonian of the form

$$H = \frac{y^2}{2} + V(x) \tag{11}$$

where y is the canonical momentum. There exists a simple (though only approximate) discretization procedure for this Hamiltonian that produces a two-dimensional phase space plot that has the form of a pair of transformation equations.

This is done by replacing the potential with a series of periodic "kicks" that approximate it in the limit of small period. Doing this, (12) becomes

$$H = \frac{y^2}{2} + V(x) \sum_{m=0}^{\infty} \delta(t - mT) \tag{12}$$

where T is the period between the kicks. Writing down Hamilton's equations gives

$$\begin{aligned} \dot{y} &= \frac{y_{n+1} - y_n}{T} = -\frac{dV(x)}{dx} \\ \dot{x} &= \frac{x_{n+1} - x_n}{T} = y_{n+1} \end{aligned} \tag{13}$$

or

$$\begin{aligned} y_{n+1} &= y_n - T\frac{dV(x)}{dx} \\ x_{n+1} &= x_n + T y_{n+1} \,. \end{aligned} \tag{14}$$

Equations (15) are the mapping equations[1] that have the approximate topology and fixed points of the phase space of the system described by H. Therefore, since it is easy to tell from a plot of a one-dimensional potential where the fixed points lie (i.e. o-points lie in valleys, x-points lie on hills), it is easy to make maps with desired stationary points using this method.

[1]In the second equation, y_{n+1} is used instead of y_n to make the map area preserving. The discretization procedure always introduces error into the system, and using y_{n+1} makes the error arise in the shape of the trajectories rather than in violation of area preservation.

Unfortunately, there are some drawbacks. First of all, since all stationary points of a Hamiltonian of this form lie on the x-axis, so must all the stationary points of this map. Second, this discretization procedure (as it does in numerical analysis) introduces error into the system which usually appears in the form of a mild stochasticity. Though all one-dimensional Hamiltonians are integrable, this is only an approximate solution so the map is only approximately integrable. In the same way, the fixed points of the map are only approximately those implied by the shape of the potential.

B. Maps with a given invariant curve: the McMillan method

Typically, one's desires for the appearance of a map go beyond just fixed points. For example, one might have a qualitative understanding of the behavior of the trajectories and might be more interested in finding a map with a given invariant curve, i.e. a curve that is mapped onto itself by the Eqs. (1). McMillan found a method for accomplishing this task for curves that are symmetric about the line $x_n = y_n$.

Suppose the function $x_n = \phi(y_n)$ represents a curve in the (x_n, y_n) plane that one wants to translate into an invariant curve. Given a pair of transformation equations of the form

$$\begin{aligned} x_{n+1} &= y_n \\ y_{n+1} &= -x_n + f(y_n) \end{aligned} \tag{15}$$

is there a function $f(y)$ that will make this map produce such a curve?

If there is and $x_n = \phi(y_n)$ is to be invariant, then it must be true that $x_{n+1} = f(y_{n+1})$. Likewise, if f is invertible it must be true that $y_n = \phi^{-1}(x_n)$ and $y_{n+1} = f^{-1}(x_{n+1})$. Substituting these into (14) and solving for $f(y_n)$ gives

$$f(y_n) = \phi(y_n) + \phi^{-1}(y_n)\ . \tag{16}$$

Therefore, if one has a curve $\phi(y_n)$ in mind, by inverting this function and using the expression (17) in the map (16), one obtains a pair of transformation equations for which the curve $\phi(y_n)$ *and its inverse* $\phi^{-1}(y_n)$ are invariant curves.

This has proved to be most effective for double-valued curves that are symmetric about the line $x = y$ (i.e. are their own inverse). If $\phi(y_n)$ is a double valued function and $\phi(y_n) = \phi^{-1}(y_n)$, the expression (17) should be treated as $f(y_n) = \phi^1(y_n) + \phi^2(y_n)$ where ϕ^1 and ϕ^2 are the two values of the function at the point y_n.

Another way to look at this situation is the following: If $f(y_n)$ is an arbitrary, single-valued, well-behaved function (that need not necessarily have a continuous derivative), then there is only one function $\phi(y_n)$ that exists such that the sum of itself and its inverse equals $f(y_n)$. In other words, f uniquely defines ϕ, though either one can be found from the other.

As an example, consider the function $f = 2ky_n/(1 + y_n^2)$. It can be shown that this function uniquely defines the double valued function $x^2y^2 + x^2 + y^2 - 2kx =$ constant as its corresponding invariant curve. The iteration of (16) for various initial conditions is shown in Fig. 2 (after McMillan), which exhibits the predicted curve.

While the McMillan method often works beautifully, as in the previous example, it too has limitations. First and most importantly, it does not guarantee integrability. Though the example just shown did generate an integrable plot, this was planned ahead of time. In general, maps that are found in this way are nonintegrable. Though the desired invariant curve is always there (guaranteed), it is often surrounded by (if not lost in) a sea of stochastic behavior.

C. Guaranteed integrability

Until now, all of the methods discussed have centered on finding maps with specified qualitative features, but nothing has been said about guaranteeing that these maps be integrable. The chances that any map picked randomly from the air is integrable is essentially zero. As it turns out, nonintegrable maps are more abundant than integrable maps to the same extent that real numbers are more abundant than rationals. Integrable maps exist but they must be found; they cannot be guessed. Therefore, the issue of finding integrable maps

is not a trivial one.

1 Classical potential method — trajectory integration

One such method has been found by us; it makes use of the fact that all one degree-of-freedom Hamiltonian systems are integrable. This method, called the "trajectory integration" method, is very similar to that discussed in Sec. 2.A.3 in that the maps it generates start from a potential. However, the discretization procedure is analytic and produces no error.

Suppose one desires a pair of iteration equations that gives a set of fixed points that all lie on the same line (preferably, the x-axis), has a desired topology, and at the same time is completely integrable. Such a map can be obtained using the following procedure:

1. Write down a one-dimensional potential $V(x)$ that would produce a set of phase space trajectories that have the same fixed points and topology as the desired mapping equations.

2. Take the function $V(x)$ and put it in the Hamiltonian $H = y^2/2 + V(x)$. Differentiate to get Hamilton's equations. Integrate these to get the coordinates x and y in terms of their initial conditions (x_0, y_0) and the time t.

3. Make the notation change $(x, y) \rightarrow (x_{n+1}, y_{n+1})$ and $(x_0, y_0) \rightarrow (x_n, y_n)$ and turn the continuous time parameter t into a discrete time step Δ.

What results is a pair of transformation equations of the form of (1) that has the exact same topology and fixed points as the phase space specified by the potential $V(x)$, and most importantly, is integrable.

Admittedly, the procedure just outlined is a little vague. However, as the following example will hopefully lucidate, the method is very simple and effective.

2 Example: The concentric circle map

Suppose the desired map is one with a stable fixed point at the origin, surrounded by a family of concentric circles. Following step 1, a potential that would produce a phase space with this topology is just a parabola $V(x) = x^2/2$. As prescribed in step 2, assembling this potential into a Hamiltonian gives $H = y^2/2 + x^2/2$. Solution of Hamilton's equations gives the following expressions for the trajectory $(x(t), y(t))$ in terms of the initial conditions and the time:

$$\begin{aligned} x(t) &= x_0 \cos(t) + y_0 \sin(t) \\ y(t) &= -x_0 \sin(t) + y_0 \cos(t) \ . \end{aligned} \tag{17}$$

Finally, making the change of notation specified in step 3 gives the map

$$\begin{aligned} x_{n+1} &= x_n \cos(\Delta) + y_n \sin(\Delta) \\ y_{n+1} &= -x_n \sin(\Delta) + y_n \cos(\Delta) \ . \end{aligned} \tag{18}$$

The constant Δ may be chosen arbitrarily and sets the step size between points on the map. The surface of section for three initial conditions is depicted in Fig. 3. As promised, the method described produced an explicit, area-preserving map with exactly the desired topology, the desired fixed point, and most importantly, unadulterated integrability.

III. Magnetostatic Applications

The use of maps as an analytic tool goes beyond just classical mechanics. Any system that can be shown to be Hamiltonian is open to analysis using these techniques. As it turns out, the field lines of a static magnetic field with one constant component can be shown to be a Hamiltonian system. The field lines play the role of phase space trajectories, the constant component of the field plays the role of the parameter (i.e. the time) and the perpendicular component of the vector potential (when scaled correctly) plays the role of the Hamiltonian. Therefore, all the tools introduced in Sec. 2 can be applied to study such magnetostatics problems.

A. Magnetic field lines as a hamiltonian system

The equations for the field lines of a static magnetic field are

$$\frac{dx}{B_x} = \frac{dy}{B_y} = \frac{dz}{B_z} , \tag{19}$$

which come from the condition $\nabla \cdot \mathbf{B} = 0$. If B_z is a constant, say B_0, the following conditions for the x and y coordinates result:

$$\frac{dx}{dz} = \frac{B_x}{B_0} , \qquad \frac{dy}{dz} = \frac{B_y}{B_0} . \tag{20}$$

The vector potential (also time-independent) can be chosen to be

$$\mathbf{A} = B_0 \psi(x,y)\, \hat{z} + B_0 x\, \hat{y} , \tag{21}$$

which is consistent with the fact that B_z is constant. Taking the curl of (22) gives

$$B_x = B_0 \frac{\partial \psi}{\partial x} , \qquad B_y = -B_0 \frac{\partial \psi}{\partial y} \tag{22}$$

and substitution of these into (21) results in the following:

$$\frac{dx}{dz} = \frac{\partial \psi}{\partial y} , \qquad \frac{dy}{dz} = -\frac{\partial \psi}{\partial x} . \tag{23}$$

Therefore, taking the z-component of the vector potential as a Hamiltonian, the x and y spatial coordinates as phase-space coordinates, and the z-coordinate as the time, a magnetostatic field forms a Hamiltonian system and is therefore suitable for study using the techniques described Sec. 2.

B. Examples of constructing field line maps

1 The tokamak field map

The concentric circle map made in Sec. 2.C.2 was chosen as an example for two reasons. First, it is the simplest example of a map that can be constructed using the trajectory

integration method. Second, it is the map that describes the helical confinement fields in a tokamak.

As shown in Fig. 4, the fields in a tokamak are helical and wind around the torus. If a poloidal plane cross-section is taken through the torus (i.e. a cut through a meridian) the intersections of the field lines with the plane would make a plot that would look like that shown in Fig. 3. Since $\mathbf{B}$ is a Hamiltonian system (as was just shown) this plot is a completely proper Hamiltonian surface of section. From Fig. 3, one can immediately identify Eqs. (19) as the map for this surface of section and $\psi = y^2/2 + x^2/2$ is the vector potential as defined in (22).

At first this map might look a little too specific and trivial. Since the argument of the sines and cosines in the map has no radial dependence, as one travels from the origin radially outward, the winding number $(\Delta/2\pi)$ is constant. However, the safety factor or "q-profile" of a tokamak $q(r)$ (which is just the inverse of the winding number) has radial dependence. Does this mean that this map is an inappropriate description?

Actually, no. Taking the map without regard to the vector potential, it may be "fine tuned" to achieve any desired q-profile. The original map is

$$\begin{aligned} x_{n+1} &= x_n \cos(\Delta) + y_n \sin(\Delta) \\ y_{n+1} &= -x_n \sin(\Delta) + y_n \cos(\Delta) \end{aligned} \tag{24}$$

and the q-profile is given by $q = 2\pi/\Delta$. From the expression $\psi = y^2/2 + x^2/2$ for the vector potential, it is easy to see that the radius is simply given by

$$r = \sqrt{2\psi}\ . \tag{25}$$

Therefore, to give q the desired r dependence, one need only give the discretization parameter ψ-dependence. The map (25) then becomes

$$\begin{aligned} x_{n+1} &= x_n \cos(\Delta(\psi)) + y_n \sin(\Delta(\psi)) \\ y_{n+1} &= -x_n \sin(\Delta(\psi)) + y_n \cos(\Delta(\psi)) \end{aligned} \tag{26}$$

Unfortunately, the map (25) is no longer the solution to the vector potential (the Hamiltonian) from which it was originally derived, but this is actually not a big problem. Giving Δ dependence on ψ effectively tunes the vector potential so that the potential $V(x)$ is no longer a parabola. Rather, it is an upward-turned well with the sides contorted to give the desired winding number.

2 The current from a potential map

At this point it is necessary to give some physical relevance to the process of creating magnetic field maps from a potential. Magnetic fields do not come from one-dimensional potentials, they come from currents, so it would be nice to have an expression for the current of a map in terms of the potential that was used to derive it.

Such an expression is easy to get since the current is just the Laplacian of the vector potential. Referring to Eq. (22) one gets

$$\nabla^2 \mathbf{A} = B_0 \left(\frac{\partial^2 \psi(x,y)}{\partial x^2} + \frac{\partial^2 \psi(x,y)}{\partial y^2} \right) \hat{z} = -\frac{4\pi}{c} \mathbf{J} \, . \tag{27}$$

Since $\psi = y^2/2 + V(x)$, the current in terms of the potential $V(x)$ is

$$\mathbf{J} = -\frac{cB_0}{4\pi} \left(\frac{\partial^2 V(x)}{\partial x^2} + 1 \right) \hat{z} \, , \tag{28}$$

where $V(x)$ always has units of length squared.

Notice that this gives the current of a parabolic potential map (i.e. the original concentric circle map) to be constant.

3 The divertor map

The trajectory integration method can be used to address the following question: "Does there exist an explicit, integrable map for the field lines in a Tokamak with a single-null divertor?" If so, it must look like that shown in Fig. 5. As stated in Sec. 2.C.1, the

prerequisite for use of the trajectory method was that all the fixed points lie on one line (i.e. the x-axis). Since the desired divertor topology satisfies this criterion, the method will work.

The first step is to find a potential that produces the above topology. It is easy to see that this will be a curve with two wells, as depicted in Fig. 6. This $V(x)$ could, however, be made in many different ways. One could use a cubic polynomial or a 4^{th} order polynomial with coefficients tailored to this shape. One could also use three parabolae spliced together so that their slopes match at the discontinuity points.

For the purposes here, the spliced parabolae will work best. This is for several reasons. First of all, use of a polynomial $V(x)$ would result in an elliptic integral for the trajectories $x(t)$ and $y(t)$, which is solvable only under restricted circumstances. Second, if parabolae are used, the result will be two concentric circle maps (connected by a separatrix map), both of which can then be modified to encompass any q-profile desired, just as the concentric circle map was earlier. The discontinuous quality of this map will unfortunately produce some algebraic difficulties down the road, but the end result will make it worth the effort.

In accordance with step 1 of the procedure, select the potential

$$V(x) = \begin{cases} \dfrac{x^2}{2} & x < x_1 \\ -\dfrac{(x-c)^2}{2} + d & x_1 \le x \le x_2 \\ \dfrac{(x-a)^2}{2} + b & x > x_2 \end{cases} , \tag{29}$$

where $x_1 = c/2$, $x_2 = \dfrac{c-a}{2}$, $c = \dfrac{a^2+4b}{2a}$, and $d = c^2/4$.

Integrating Hamilton's equations must be done for each of the three regions of the potential. The trajectories in terms of the initial conditions and time are for $x < x_1$:

$$\begin{aligned} x(t) &= x_0 \cos(t) + y_0 \sin(t) \\ y(t) &= -x_0 \sin(t) + y_0 \cos(t) \ , \end{aligned} \tag{30a}$$

for $x_1 < x < x_2$:

$$\begin{aligned} x(t) &= (x_0 - c)\cosh(t) + y_0 \sinh(t) + c \\ y(t) &= -(x_0 - c)\sinh(t) + y_0 \cosh(t) \ , \end{aligned} \tag{30b}$$

and for $x > x_2$:

$$\begin{aligned} x(t) &= (x_0 - a)\cos(t) + y_0 \sin(t) + a \\ y(t) &= -(x_0 - a)\sin(t) + y_0 \cos(t) \ . \end{aligned} \tag{30c}$$

The next step is to discretize these equations. Step 3 of the procedure outlined in Sec. 2.C.1 called for turning the time parameter t into a discrete time step Δ. Unfortunately, because of the discontinuous quality of this potential, this discretization procedure does not quite work. To see why, let's follow through with the procedure, see where it fails and then fix it. Replacing t with Δ gives the discontinuous map for $x_n > x_2$:

$$\begin{cases} x_{n+1} = (x_n - a)\cos(\Delta) + y_n \sin(\Delta) + a \\ y_{n+1} = -(x_n - a)\sin(\Delta) + y_n \cos(\Delta) \end{cases} \tag{31a}$$

for $x_1 < x_n < x_2$:

$$\begin{cases} x_{n+1} = (x_n - c)\cosh(\Delta) + y_n \sinh(\Delta) + c \\ y_{n+1} = -(x_n - c)\sinh(\Delta) + y_n \cosh(\Delta) \end{cases} \tag{31b}$$

and for $x_n > x_2$:

$$\begin{cases} x_{n+1} = (x_n - a)\cos(\Delta) + y_n \sin(\Delta) + a \\ y_{n+1} = -(x_n - a)\sin(\Delta) + y_n \cos(\Delta) \ . \end{cases} \tag{31c}$$

At first glance this might look like the integrable divertor map desired (i.e. two circles with an x-point in between) but such is not the case. Consider an initial condition chosen near the fixed point $(x, y) = (c, 0)$ as shown in Fig. 7. By inspection of Fig. 7, one sees that the point follows the central iteration for slightly "too long," thereby flying off the desired invariant curve. The trajectory crosses the discontinuity point x_1 at some time in the middle

of the time period Δ, but it does not begin to follow the $x < x_1$ map until the *end* of the time period. Part of the time period Δ should be spent in the central map and part should be spent in the left map, however, Eqs. (30) apply the central map on the entire time interval. Therefore, this map is wrong.

To correct this problem, it is necessary to find what portion of the time period Δ should spent in the central region, what portion should be spent in the left region, and apply the correct amount of time to each map. To do this, one needs to do the following: Suppose x_n and y_n are the coordinates right before the jump over the discontinuity is made, and x_{n+1} and y_{n+1} are the coordinates after the jump is made (as drawn in Fig. 7) using the map for the center region. At some time t (which is less than Δ), the trajectory passes through the discontinuity point (x_1, y_1) where

$$y_1 = -\sqrt{(x_1 - c)^2 - (x_n - c)^2 + y_n^2} \tag{32}$$

and x_1 is as defined in (30). Since the time between (x_n, y_n) and (x_1, y_1) is t, it must be true that

$$\begin{aligned} x_1 &= (x_n - c)\cosh(t) + y_n \sinh(t) + c \\ y_1 &= -(x_n - c)\sinh(t) + y_n \cosh(t) \end{aligned} \tag{33}$$

since t is spent in the central region. Using the first expression in the second to eliminate the sinh, one gets an expression for t

$$t = \cosh^{-1}\left[\frac{(x_1 - c)(x_n - c) - y_1 y_n}{(x_n - c)^2 - y_n^2}\right] . \tag{34}$$

This t represents the amount of time to get from the point (x_n, y_n) to the discontinuity point (x_1, y_1). Since the entire time period of the iteration is Δ, the time spent in the next map (that for $x < x_1$) is just $\Delta - t$. Therefore, the point (x_{n+1}, y_{n+1}) should not be that defined by (30). Rather, it should be the following:

$$\begin{aligned} x_{n+1} &= x_1 \cos(\Delta - 1) + y_1 \sin(\Delta - t) \\ y_{n+1} &= -x_1 \sin(\Delta - t) + y_1 \cos(\Delta - t) . \end{aligned} \tag{35}$$

In other words, since the portion of the iteration interval Δ that is spent in the central region is t, the portion of the interval that is spent in the left region is $\Delta - t$, and Eq. (34) just represents the application of this "leftover" time to the left map.

For points that do not cross a discontinuity, this procedure is not necessary and Eqs. (30) work fine. However, for those that do cross, the time must be split in two and applied to two different maps. Since the potential (30) has two discontinuities, there will be four different expressions for crossing iterations, since the two discontinuities can be crossed in either direction. Therefore, adding in the three original maps given in (29), the resulting map is a seven part discontinuous, integrable, area-preserving, explicit map that gives exactly the topology and fixed points originally set as a goal. The map, written out explicitly, is the following:

For $(x_n - c)\cosh\Delta + y_n \sinh\Delta + c < x_1 < x_n$:

$$x_{n+1} = x_1 \cos(\Delta - 1) + y_1 \sin(\Delta - t)$$
$$y_{n+1} = -x_1 \sin(\Delta - t) + y_1 \cos(\Delta - t) \ .$$

where

$$t = \cosh^{-1}\left[\frac{(x_1 - c)(x_n - c) - y_1 y_n}{(x_n - c)^2 - y_n^2}\right] \qquad \text{and} \qquad y_1 = -\sqrt{(x_1 - c)^2 - (x_n - c)^2 + y_n^2}$$

For $x_n < x_1$ and $x_n \cos\Delta + y_n \sin\Delta < x_1$:

$$x_{n+1} = x_n \cos(\Delta) + y_n \sin(\Delta)$$
$$y_{n+1} = -x_n \sin(\Delta) + y_n \cos(\Delta) \ .$$

For $x_n < x_1 < x_n \cos\Delta + y_n \sin\Delta$:

$$x_{n+1} = (x_1 - c)\cosh(\Delta - t) + y_1 \sinh(\Delta - t) + c$$
$$y_{n+1} = -(x_1 - c)\sinh(\Delta - t) + y_1 \cosh(\Delta - t) \ .$$

where

$$t = \cos^{-1}\left[\frac{x_1 x_n - y_1 y_n}{x_n^2 + y_n^2}\right] \quad \text{and} \quad y_1 = \sqrt{x_n^2 - x_1^2 + y_n^2}$$

For $x_1 < x_n$ and $(x_n - c)\cosh\Delta + y_n \sinh\Delta + c < x_2$:

$$x_{n+1} = (x_n - c)\cosh(\Delta) + y_n \sinh(\Delta) + c$$
$$y_{n+1} = -(x_n - c)\sinh(\Delta) + y_n \cosh(\Delta) \ .$$

For $x_n < x_2 < (x_n - c)\cosh\Delta + y_n \sinh\Delta + c$:

$$x_{n+1} = (x_2 - a)\cos(\Delta - t) + y_2 \sin(\Delta - t) + a$$
$$y_{n+1} = -(x_2 - a)\sin(\Delta - t) + y_2 \cos(\Delta - t) \ .$$

where

$$t = \cosh^{-1}\left[\frac{x_2 - c)(x_n - c) - y_2 y_n}{(x_n - c)^2 - y_n^2}\right] \quad \text{and} \quad y_2 = \sqrt{(x_2 - c)^2 - (x_n - c)^2 + y_n^2} \ .$$

For $x_n > x_2$ and $(x_n - a)\cos\Delta + y_n \sin\Delta + a > x_2$:

$$x_{n+1} = (x_n - a)\cos(\Delta) + y_n \sin(\Delta) + a$$
$$y_{n+1} = -(x_n - a)\sin(\Delta) + y_n \cos(\Delta) \ .$$

For $(x_n - a)\cos\Delta + y_n \sin\Delta + a < x_2 < n_n$:

$$x_{n+1} = (x_2 - c)\cosh(\Delta - t) + y_2 \sinh(\Delta - t) + c$$
$$y_{n+1} = -(x_2 - c)\sinh(\Delta - t) + y_2 \cosh(\Delta - t) \ .$$

where

$$y_2 = -\sqrt{(x_n - 1)^2 - (x_2 - a)^2 + y_n^2} \quad \text{and} \quad t = \cos^{-1}\left[\frac{x_2 - a)(x_n - a) - y_2 y_n}{(x_n - a)^2 - y_n^2}\right] \ .$$

The plot that results from this map is shown in Fig. 8. Note that using the procedure of making Δ a function of ψ, any desired q-profile may be put in either circular region. Similarly, the step size may be changed along the separatrix.

IV. Closing Comments

Now that a divertor map has been found, perturbations may be added to see how different current arrangements break up the confinement surfaces. To add a perturbation, a function with a small-parameter multiplier with z-dependence should be added to the vector potential and then propagated through to the map. Future plans include looking at such perturbations on the divertor map, with particular interest in exploring the possibility of using of an ergodic limiter with a divertor arrangement. Also, a method similar to trajectory integration that produces *any* map topology rather than one for which all fixed points lie on the same line is currently being explored. If such a method is found, this method will prove to be much more general and useful.

References

[1]M. Tabor, *Chaos and Integrability in Classical Mechanics* (Wiley, New York, 1989).

[2]A. Lichtenberg and M. Lieberman, *Regular and Stochastic Motion* (Springer-Verlag, New York, 1983).

[3]M. Henon and C. Heiles, Astron. J. **69**, 73 (1964).

[4]E. McMillan, in *Topics in Modern Physics: A Tribute to E.U. Condon* (Colorado Assoc. Univ. Press, Boulder, 1971) p. 219.

Appendix—Perturbations on Magnetic Fields

In the real world, integrable systems do not exist. As was said earlier, nonintegrable systems (maps, in the earlier context) are more common than integrable systems to the same extent that real numbers are more common than rational numbers. Though in principle a system that obeys Newton's laws has the capacity to be integrable, it is only infinitesimally likely that any given system will be. Just as the probability of randomly selecting an integer from the real number line is zero, the probability of any naturally-occurring system being integrable is zero.

This then raises the question, "Once you've found an integrable map, what good does it do you if it doesn't describe any real system?" Well, there are two obvious answers. The first answer is that many systems are approximately integrable, and integrable maps are generally easier to analyze than stochastic maps.

The second, more immediately relevant answer is that it is very informative to see how integrable maps behave under perturbations. Suppose you have an integrable Hamiltonian H_0 for which you have solved the trajectories and have found a descriptive Poincáre map. If you take a small (nonintegrable) perturbation Hamiltonian H', apply it to this system and propagate the perturbation into the map, the invariant surfaces will break up into fixed point chains (as dictated by the Poincáre-Birkhoff theorem). The integrable map will have become weakly stochastic.

In this case, one can definitively say that the stochasticity seen in the perturbed map comes from the addition of the perturbation Hamiltonian alone and has no basis in the original system. That is, since the unperturbed system exhibited no stochastic behavior, the stochasticity in the perturbed system can be considered the net effect of adding the perturbation. Because of this, one can separately make definite statements about the behavior of

H' (i.e. how it affects integrable maps), and of H_0 (i.e. how it behaves under perturbations). If the map were originally stochastic and H' just caused some broadening of the irregular regions, one would have a harder time attributing specific behavior (instabilities etc.) to the H' and H_0 independently.

The purpose of this appendix is to present a method for propagating a perturbation H' into the map of a solved, integrable system H_0. Since the immediate applications of this method will be in magnetostatics, H_0 will be taken to be ψ, the (scaled) perpendicular component of a vector potential and (x, y) are phase space coordinates (see last section).

Consider the vector potential

$$\mathbf{A}_0 = B_0\psi(x,y)\,\hat{z} + B_0 x\,\hat{y} \tag{A.1}$$

and an arbitrary perturbation potential

$$\varepsilon\mathbf{A}_1 = \varepsilon A_x^1\hat{x} + \varepsilon A_y^1\hat{y} + \varepsilon A_z^1\hat{z} \qquad \varepsilon\mathbf{B}_1 = \nabla\times(\varepsilon\mathbf{A}_1)\ . \tag{A.2}$$

Assume that $\mathbf{A}_0$ is integrable and that ε is a small, dimensionless parameter.
The unperturbed magnetic field is

$$\nabla\times\mathbf{A}_0 = B_0\frac{\partial\psi}{\partial y}\,\hat{x} - B_0\frac{\partial\psi}{\partial x}\,\hat{y} + B_0\hat{z} = \mathbf{B}_0\ . \tag{A.3}$$

In Sec. 3 it was shown that the field line equations take the form of Hamilton's equations

$$\frac{dx}{dz} = \frac{\partial\psi(x,y)}{\partial y}\ , \qquad \frac{dy}{dz} = -\frac{\partial\psi(x,y)}{\partial x} \tag{A.4}$$

so if $\mathbf{B}_0$ is perturbed, there results a net (nonintegrable) magnetic field

$$\mathbf{B} = \nabla\times\mathbf{A} \equiv \nabla\times\mathbf{A}_0 + \nabla\times\mathbf{A}_1\ , \tag{A.5}$$

Hamilton's equations (A.4) become the following:

$$\frac{dy}{dz} = \frac{B_0\dfrac{\partial\psi}{\partial y} + \varepsilon\left(\dfrac{\partial A_z^1}{\partial y} - \dfrac{\partial A_y^1}{\partial z}\right)}{B_0 + \varepsilon\left(\dfrac{\partial A_y^1}{\partial x} - \dfrac{\partial A_x^1}{\partial y}\right)} \tag{A.6a}$$

$$\frac{dy}{dz} = \frac{-B_0 \dfrac{\partial \psi}{\partial x} + \varepsilon \left(\dfrac{\partial A_x^1}{\partial z} - \dfrac{\partial A_z^1}{\partial x} \right)}{B_0 + \varepsilon \left(\dfrac{\partial A_y^1}{\partial x} - \dfrac{\partial A_x^1}{\partial y} \right)} \,. \tag{A.6b}$$

Here the A^1's are the components of the perturbation potential as defined earlier. From now on, the combination of derivatives of the A^1's will be referred to as components of the perturbation field $\mathbf{B}_1$ (as defined in (A.2).

To simplify these expressions, binomial expand the denominator (the same in both (A.6a) and (A.6b)).

$$(B_0 + \varepsilon B_z')^{-1} = \frac{1}{B_0} \left[1 + \varepsilon \left(\frac{B_z'}{B_0} \right) \right]^{-1} = \frac{1}{B_0} \left[1 - \varepsilon \left(\frac{B_z'}{B_0} \right) + \varepsilon^2 \left(\frac{B_z'}{B_0} \right)^2 + \cdots \right] \,. \tag{A.7}$$

Discarding all but linear terms gives

$$\frac{dx}{dz} = \frac{\partial \psi}{\partial y} + \varepsilon \left(\frac{B_x'}{B_0} - \frac{\partial \psi}{\partial y} \frac{B_z'}{B_0} \right) \tag{A.8a}$$

$$\frac{dy}{dz} = \frac{\partial \psi}{\partial y} + \varepsilon \left(\frac{B_y'}{B_0} - \frac{\partial \psi}{\partial y} \frac{B_z'}{B_0} \right) \,. \tag{A.8b}$$

Therefore, to linear order in ε, the perturbation takes the form of two functions added onto the end of the original (solved) pair of unperturbed Hamilton's equations.

Since the unperturbed trajectories $x(z)$ and $y(z)$ are already known, it would be convenient to have two functions (say, $x_1(z)$ and $y_1(z)$) that could be solved for separately that would constitute a linear correction to these trajectories. To get an equation for these, first make the notation change $(x(z), y(z)) \rightarrow (x_0(z), y_0(z))$ and call the perturbed solution $(x(z), y(z))$. In terms of these, Eqs. (A.4) become

$$\frac{dx_0(z)}{dz} = \frac{\partial \psi(x_0, y_0)}{\partial y_0(z)} \quad \text{and} \quad \frac{dy_0(z)}{dz} = -\frac{\partial \psi(x_0, y_0)}{\partial x_0(z)} \,. \tag{A.9}$$

Now express the perturbed trajectory as a series in powers of ε of the form

$$\begin{aligned} x(z) &= x_0(z) + \varepsilon x_1(z) + \varepsilon^2 x_2(z) + \cdots \\ y(z) &= y_0(z) + \varepsilon y_1(z) + \varepsilon^2 y_2(z) + \cdots \,. \end{aligned} \tag{A.10}$$

Substituting these into Eqs. (A.8) gives

$$\frac{d(x_0+\varepsilon x_1)}{dz} = \frac{\partial\psi(x,y)}{\partial y} + \varepsilon\left(\frac{B'_x}{B_0} - \frac{\partial\psi}{\partial y}\frac{B'_z}{B_0}\right)$$

which, expanded out, becomes

$$\frac{dx_0}{dz} + \varepsilon\frac{dx_1}{dz} = \frac{\partial\psi(x_0,y_0)}{\partial y_0} + \frac{\partial^2\psi(x_0,y_0)}{\partial y_0^2}(\varepsilon x_1) + \varepsilon\left(\frac{B'_x}{B_0} - \frac{\partial\psi(x_0,y_0)}{\partial y_0}\frac{B'_z}{B_0}\right) + \mathcal{O}(\varepsilon^2)\ .$$

Using Eqs. (A.9) and dropping higher order terms gives

$$\frac{dx_1}{dz} = \frac{\partial^2\psi}{\partial y_0^2}y_1 + \frac{\partial^2\psi}{\partial y_0\,\partial x_0}x_1 + \left(\frac{B'_x(x_0,y_0)}{B_0} - \frac{\partial\psi}{\partial y_0}\frac{B'_z(x_0,y_0)}{B_0}\right) \tag{A.11a}$$

$$\frac{dy_1}{dz} = \frac{\partial^2\psi}{\partial x_0^2}x_1 + \frac{\partial^2\psi}{\partial x_0\,\partial y_0}y_1 + \left(\frac{B'_x(x_0,y_0)}{B_0} - \frac{\partial\psi}{\partial x_0}\frac{B'_z(x_0,y_0)}{B_0}\right) \tag{A.11b}$$

Since the functions x_0 and y_0 are known, Eqs. (A.11) are a pair of coupled ODE's which may be solved (somehow) for the trajectories x_1 and y_1.

It remains now to do the hard part: actually applying these equations to a system and solving. Thus we are poised for future work.

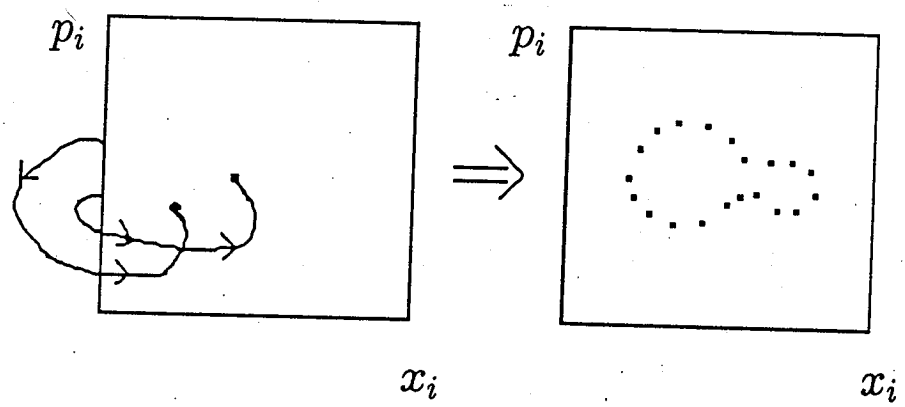

Fig. 1 Poincáre Section

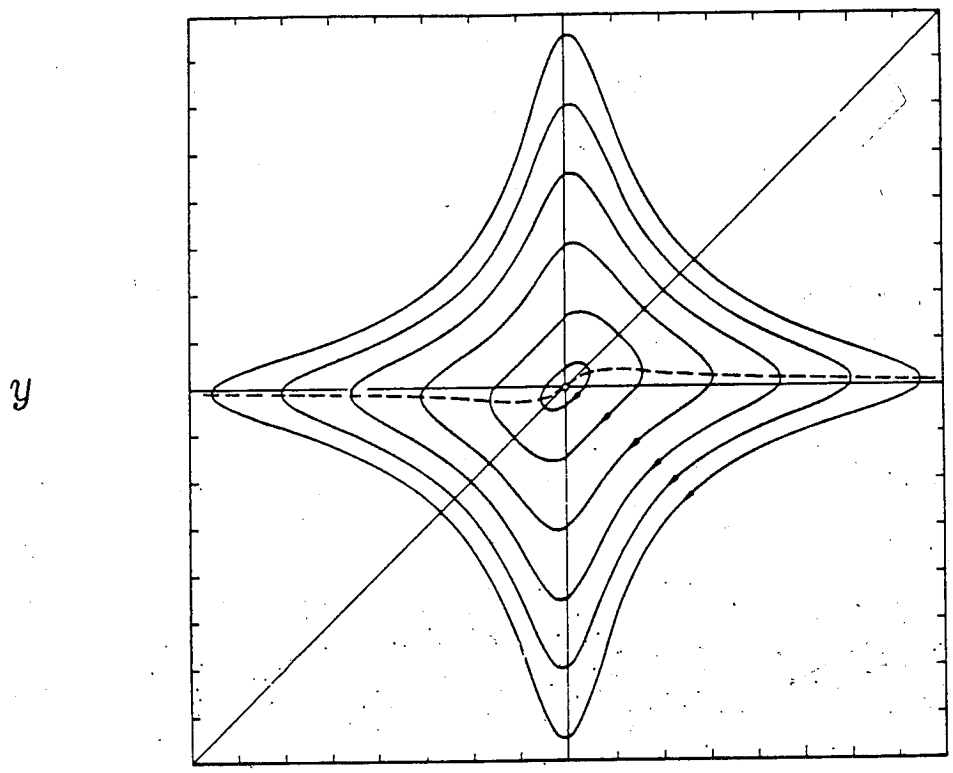

Fig. 2 McMillan Map

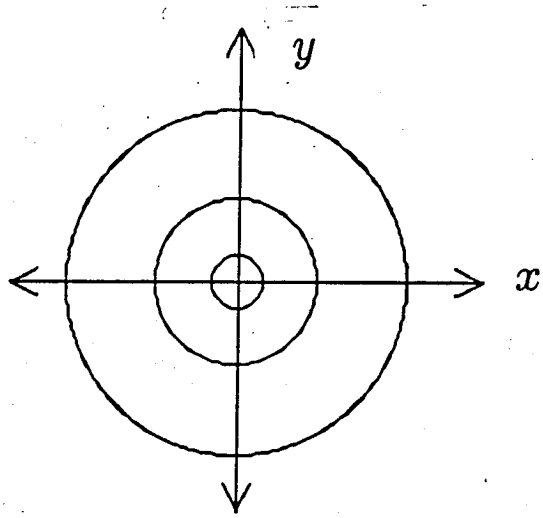

Fig. 3 Concentric Circle Map

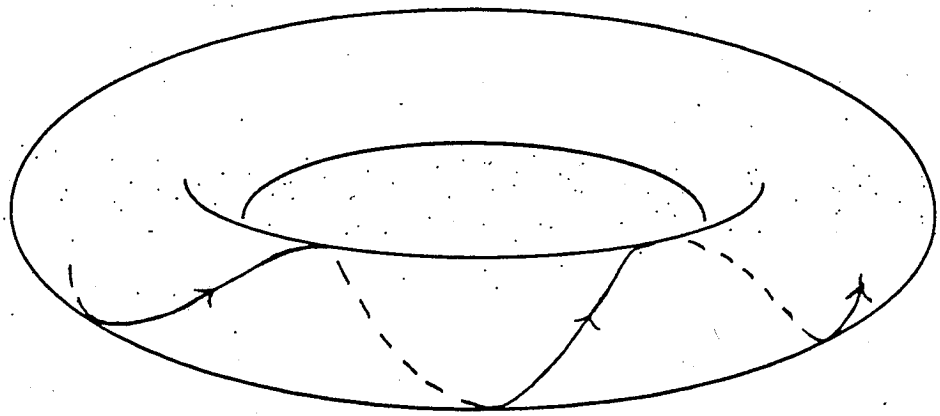

Fig. 4 Tokamak Field Line Configuration

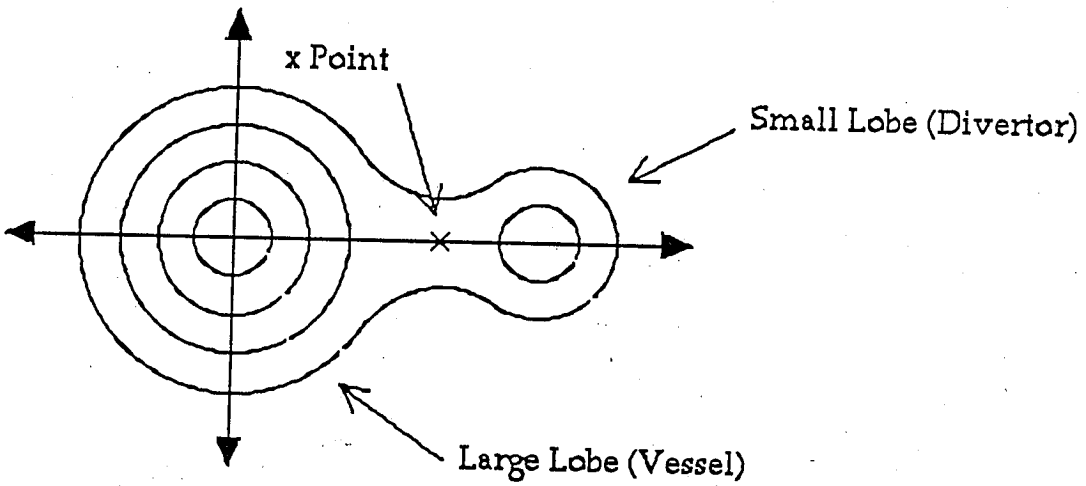

Fig. 5 Desired Divertor Map Topology

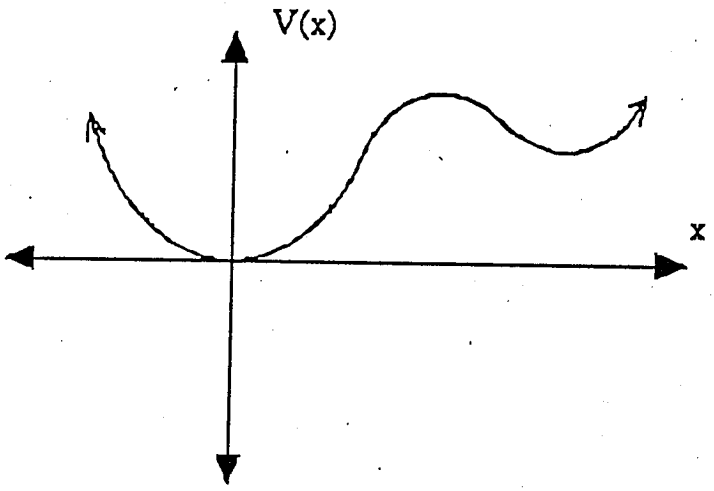

Fig. 6 Divertor Potential

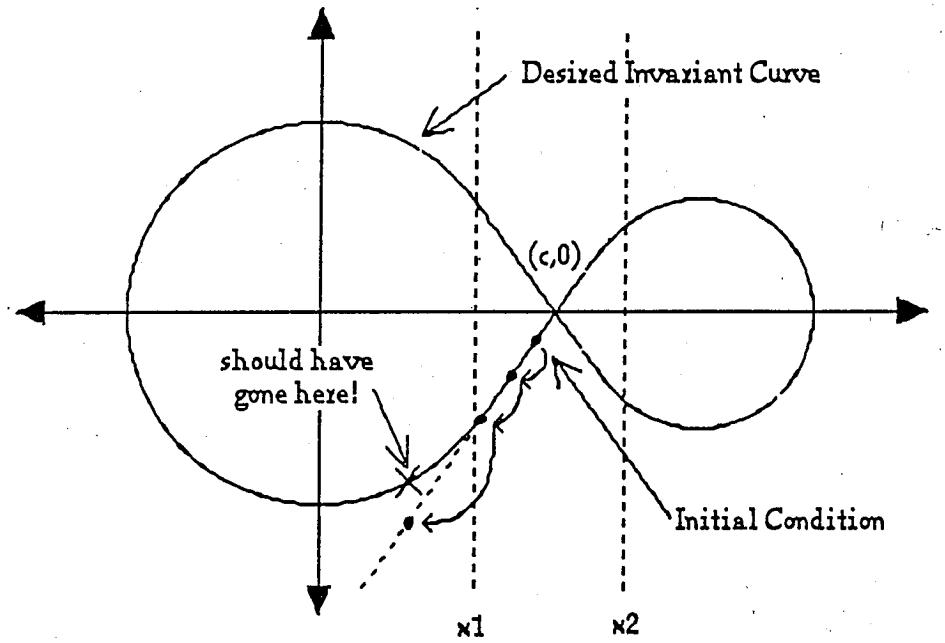

Fig. 7 Evaluation of an Initial Condition Near x-point

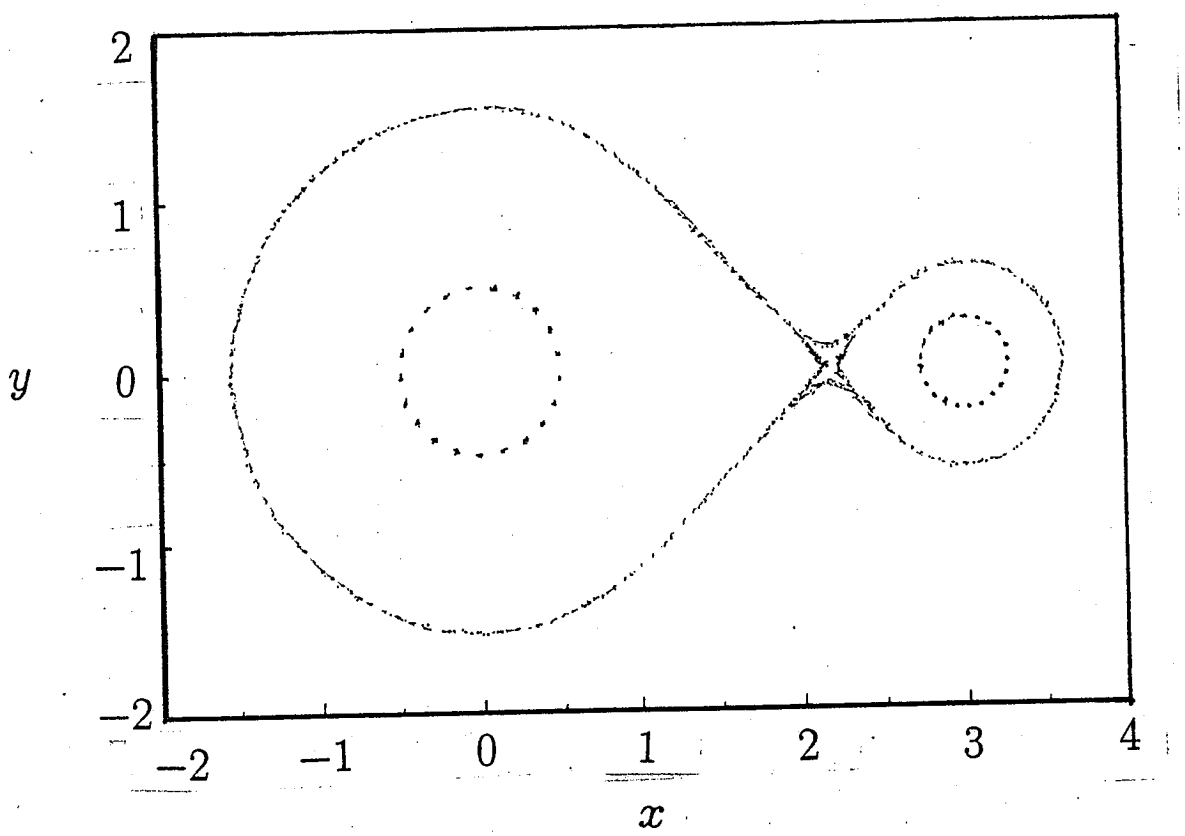

Fig. 8 Divertor Map